



Projected wave function study of \mathbb{Z}_2 spin liquids on the kagome lattice for the spin- $\frac{1}{2}$ quantum Heisenberg antiferromagnet

Yasir Iqbal,¹ Federico Becca,² and Didier Poilblanc¹

¹*Laboratoire de Physique Théorique UMR-5152, CNRS and Université de Toulouse, F-31062 France*

²*Democritos National Simulation Center, Istituto Officina dei Materiali del CNR and Scuola Internazionale Superiore di Studi Avanzati (SISSA), Via Bonomea 265, I-34136 Trieste, Italy*

(Received 6 May 2011; revised manuscript received 7 June 2011; published 20 July 2011)

Motivated by recent density-matrix renormalization group (DMRG) calculations [Yan, Huse, and White, *Science* **332**, 1173 (2011)], which claimed that the ground state of the nearest-neighbor spin-1/2 Heisenberg antiferromagnet on the kagome lattice geometry is a fully gapped spin liquid with numerical signatures of \mathbb{Z}_2 gauge structure, and a further theoretical work [Lu, Ran, and Lee, *Phys. Rev. B* **83**, 224413 (2011)], which gave a classification of all Schwinger-fermion mean-field fully symmetric \mathbb{Z}_2 spin liquids on the kagome lattice, we have thoroughly studied Gutzwiller-projected fermionic wave functions by using quantum variational Monte Carlo techniques, hence implementing exactly the constraint of one fermion per site. In particular, we investigated the energetics of all \mathbb{Z}_2 candidates (gapped and gapless) that lie in the neighborhood of the energetically competitive U(1) gapless spin liquids. By using a state-of-the-art optimization method, we were able to conclusively show that the U(1) Dirac state is remarkably stable with respect to all \mathbb{Z}_2 spin liquids in its neighborhood, and in particular for opening a gap toward the so-called $\mathbb{Z}_2[0, \pi]\beta$ state, which was conjectured to describe the ground state obtained by the DMRG method. Finally, we also considered the addition of a small second nearest-neighbor exchange coupling of both antiferromagnetic and ferromagnetic type, and obtained similar results, namely, a U(1) Dirac spin-liquid ground state.

DOI: [10.1103/PhysRevB.84.020407](https://doi.org/10.1103/PhysRevB.84.020407)

PACS number(s): 75.10.Kt, 75.10.Jm, 75.40.Mg

Introduction. The nearest-neighbor (NN) spin-1/2 quantum Heisenberg antiferromagnet (QHAF) on the kagome lattice provides ideal conditions for the amplification of quantum fluctuations and a consequent stabilization of an exotic magnetically disordered ground state, which may be a valence-bond crystal (VBC)^{1–5} or a spin liquid (SL) with fractionalized excitations.^{6–8} Recent experiments have unanimously pointed toward a SL behavior,^{9–16} in particular, Raman spectroscopic data on a nearly perfect spin-1/2 kagome compound with Heisenberg couplings (the so-called Herbertsmithite) suggested a gapless (algebraic) SL.¹⁷ On the theoretical side, the question is still wide open and intensely debated. On the one hand, series expansion provided evidence that a VBC with a 36-site unit cell has lower energy than other proposed competing states.⁴ On the other hand, it was shown that within the class of Gutzwiller-projected fermionic wave functions, a particular algebraic SL, the so-called U(1) Dirac state, has a competing energy.¹⁸ Its properties were studied in detail in Ref. 19 and it was argued that it can be a stable SL state. However, a recent DMRG study⁸ has challenged the above results, and proposed that the ground state can be a fully gapped \mathbb{Z}_2 SL with a substantially lower energy as compared to both the above estimates.

The \mathbb{Z}_2 SLs have the nice property that they are stable mean-field states and can survive quantum fluctuations. Hence, they are more likely to occur as real physical SLs, and one can safely use the projective symmetry group classification of \mathbb{Z}_2 SLs beyond mean-field level.²⁰ This complete classification of fully symmetric \mathbb{Z}_2 SLs on the kagome lattice was recently done in Ref. 21 within the Schwinger-fermion mean-field theory, resulting in an enumeration of a total of 20 \mathbb{Z}_2 mean-field states. Their main result was the identification of a *unique* gapped \mathbb{Z}_2 SL (called the $\mathbb{Z}_2[0, \pi]\beta$ state) in the neighborhood of the U(1) Dirac state. Since the U(1) Dirac SL state has the best

variational energy among the class of U(1) gapless SLs, in Ref. 21, it has been conjectured that the $\mathbb{Z}_2[0, \pi]\beta$ state may describe the ground state that has been numerically observed in the DMRG study.⁸

In this paper, we thoroughly investigate the possibility of any of these \mathbb{Z}_2 SLs being stabilized as the ground state of the NN spin-1/2 QHAF, with a particular emphasis on the $\mathbb{Z}_2[0, \pi]\beta$ state. In practice, we compute the energy of optimized variational wave functions that are constructed by applying the Gutzwiller projector to different states obtained from mean-field Hamiltonians of Schwinger fermions. In this respect, by an exact treatment of the full projector that ensures the one fermion per site constraint, we go much beyond the simple mean-field approach of Ref. 21. We calculate the energies of all \mathbb{Z}_2 SLs which can be realized up to 3rd NN in mean-field *Ansatz* and have a nonvanishing 1st NN mean-field bond. Only 12 of the 20 \mathbb{Z}_2 SLs satisfy these criteria, and all of them are continuously connected to some U(1) gapless SL.²¹ Our main result is that, contrary to what has been proposed in Ref. 21, the $\mathbb{Z}_2[0, \pi]\beta$ state has a higher energy than the gapless U(1) Dirac SL, or in other words, the U(1) Dirac SL is remarkably stable with respect to opening of a gap and consequently destabilizing into the $\mathbb{Z}_2[0, \pi]\beta$ state. We also find that all gapped \mathbb{Z}_2 SLs in the neighborhood of another competing gapless state, the uniform resonating-valence bond (RVB) state, have higher energies. Moreover, we find that all \mathbb{Z}_2 SLs have higher energy than the gapless SL states in whose neighborhoods they lie.

Model and wave function. The Hamiltonian for the NN spin-1/2 Heisenberg model is

$$\hat{\mathcal{H}} = J \sum_{\langle ij \rangle} \hat{\mathbf{S}}_i \cdot \hat{\mathbf{S}}_j, \quad (1)$$

where $\langle ij \rangle$ denote sums over NN sites and \hat{S}_i is the spin-1/2 operator at site i . All energies will be given in units of J .

The variational wave functions are defined by projecting noncorrelated fermionic states:

$$|\Psi_{\text{VMC}}(\chi_{ij}, \Delta_{ij}, \mu, \zeta)\rangle = \mathcal{P}_G |\Psi_{\text{MF}}(\chi_{ij}, \Delta_{ij}, \mu, \zeta)\rangle, \quad (2)$$

where $\mathcal{P}_G = \prod_i (1 - n_{i,\uparrow} n_{i,\downarrow})$ is the full Gutzwiller projector enforcing the one fermion per site constraint. Here, $|\Psi_{\text{MF}}(\chi_{ij}, \Delta_{ij}, \mu, \zeta)\rangle$ is the ground state of mean-field Hamiltonian containing chemical potential, hopping, and *singlet* pairing terms:

$$\begin{aligned} \mathcal{H}_{\text{MF}} = & \sum_{i,j,\alpha} (\chi_{ij} + \mu \delta_{ij}) c_{i,\alpha}^\dagger c_{j,\alpha} \\ & + \sum_{i,j} \{ (\Delta_{ij} + \zeta \delta_{ij}) c_{i,\uparrow}^\dagger c_{j,\downarrow}^\dagger + \text{H.c.} \}, \end{aligned} \quad (3)$$

where $\chi_{ij} = \chi_{ji}^*$ and $\Delta_{ij} = \Delta_{ji}$. Besides the chemical potential μ , we will also consider real and imaginary components of on-site pairing, which are absorbed in ζ . We briefly mention that a somewhat similar approach, based upon a bosonic representation of the spin operators (i.e., through Schwinger bosons), has been also used recently.²² In the latter case, however, the bosonic nature of quasiparticle operators implies that one has to deal with permanents instead of determinants, which makes the numerical calculations much heavier than in our fermionic case.

Different SL phases correspond to different patterns of distribution of χ_{ij} and Δ_{ij} on the lattice links, along with the specification of the on-site terms μ and ζ . Then, a complete specification of a SL state up to n th NN amounts to specifying the SU(2) flux through closed loops along with the optimized hopping and pairing parameters at each geometrical distance.^{20,23} These parameters are the *Ansätze* of a given state and serve as the variational parameters in the physical wave function that are optimized within the variational Monte Carlo scheme to find the energetically best state. It is worth mentioning that we use a sophisticated implementation of the stochastic reconfiguration (SR) optimization method,^{24,25} which allows us to obtain an extremely accurate determination of variational parameters. Indeed, small energy differences are effectively computed by using a correlated sampling, which makes it possible to strongly reduce statistical fluctuations. The current problem of the study of the instability of a U(1) Dirac SL state toward the $\mathbb{Z}_2[0,\pi]\beta$ state will clearly demonstrate the power of this method to capture the essential subtleties.

Results. We performed our variational calculations on a 432-site cluster with mixed periodic-antiperiodic boundary conditions which ensures nondegenerate wave functions at half-filling. The large size of the cluster ensures that the spatial modulations induced in the observables by breaking of rotational symmetry (due to mixed boundary conditions) remain smaller than the uncertainty in the Monte Carlo simulations.

Among the class of NN fully symmetric and gapless SLs, the U(1) Dirac state has the lowest energy. Its energy per site is $E/J = -0.42863(2)$, and its *Ansatz* is given by the sign convention for NN bonds in Fig. 1. Due to the U(1) flux φ being 0 and π [$\exp(i\varphi) = \prod_{\text{plaquette}} \chi_{ij}$] through triangles and hexagons, respectively, it is denoted as $[0,\pi]$. Another

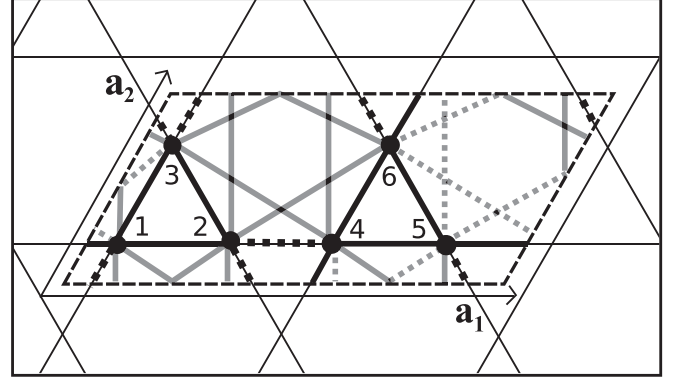


FIG. 1. The $\mathbb{Z}_2[0,\pi]\beta$ SL *Ansatz*; black (grey) bonds denote 1st NN real hopping (2nd NN real hopping and real spinon pairing) terms; solid (dashed) black bonds have $s_{ij} = 1$ (-1), solid (dashed) grey bonds have $v_{ij} = 1$ (-1), see Eq. (4). The 1st NN (2nd NN) mean-field *Ansatz* is written as $U_{(ij)} = \pm \sigma_3 [U_{\langle ij \rangle}] = \pm (\chi_2 \sigma_3 + \Delta_2 \sigma_1)$. The SU(2) flux P , through elementary triangles (e.g., 123) is $P_{123} = \sigma_3$, and that through triangles formed by two 1st NN and one 2nd NN bonds (e.g., 234) is $P_{234} = -(\chi_2 \sigma_3 + \Delta_2 \sigma_1)$. Their commutator is nonzero, $[P_{123}, P_{234}] = (-2i \sigma_2) \Delta_2$. Hence, a finite Δ_2 breaks the U(1) gauge structure down to \mathbb{Z}_2 , and opens up an energy gap via the Anderson-Higgs mechanism.^{20,23}

competing state, the NN uniform RVB state has zero flux through any plaquette and is therefore denoted as $[0,0]$; its energy per site is $E/J = -0.41216(1)$.^{18,19}

The study in Ref. 21 identified four \mathbb{Z}_2 SLs in the neighborhood of the $[0,\pi]$ state; only one of them, the $\mathbb{Z}_2[0,\pi]\beta$ state, was found to be gapped (via the 2nd NN spinon pairing term). Its *Ansatz* up to 2nd NN mean-field bond is reproduced in Fig. 1.²¹ In a suitable gauge, its mean-field *Ansatz* is specified by five real parameters. These parameters are the 1st NN real hopping (χ_1), 2nd NN real hopping (χ_2), 2nd NN real spinon pairing (Δ_2), and two onsite terms, one for the chemical potential μ and the other for the real on-site pairing ζ_R . The mean-field Hamiltonian can be then conveniently cast in the following form:

$$\begin{aligned} \mathcal{H}_{\text{MF}}\{\mathbb{Z}_2[0,\pi]\beta\} = & \chi_1 \sum_{\langle ij \rangle, \alpha} s_{ij} c_{i,\alpha}^\dagger c_{j,\alpha} + \sum_{\langle\langle ij \rangle\rangle} v_{ij} \left\{ \chi_2 \sum_{\alpha} c_{i,\alpha}^\dagger c_{j,\alpha} \right. \\ & \left. + \Delta_2 (c_{i,\uparrow}^\dagger c_{j,\downarrow}^\dagger + \text{H.c.}) \right\} + \sum_i \left\{ \mu \sum_{\alpha} c_{i,\alpha}^\dagger c_{i,\alpha} \right. \\ & \left. + \zeta_R (c_{i,\uparrow}^\dagger c_{i,\downarrow}^\dagger + \text{H.c.}) \right\}, \end{aligned} \quad (4)$$

where $\langle ij \rangle$ and $\langle\langle ij \rangle\rangle$ denote sums over 1st and 2nd NN sites, respectively. s_{ij} and v_{ij} encode the sign structure of the 1st and 2nd NN bonds, respectively, as shown in Fig. 1. The 1st NN real hopping (χ_1) will be taken as a reference, and hence set to unity hereafter. The physical variational wave function of this SL state then depends on four variational parameters, $|\Psi_{\text{VMC}}(\chi_2, \Delta_2, \mu, \zeta_R)\rangle = \mathcal{P}_G |\Psi_{\text{MF}}(\chi_2, \Delta_2, \mu, \zeta_R)\rangle$.

For a generic unbiased starting point in the four-dimensional variational space, the variation of parameters and energy in the SR optimization is shown in Fig. 2. As one can clearly see, the energy converges neatly [see point B in Fig. 2(b)] to the reference value of the suitably extended

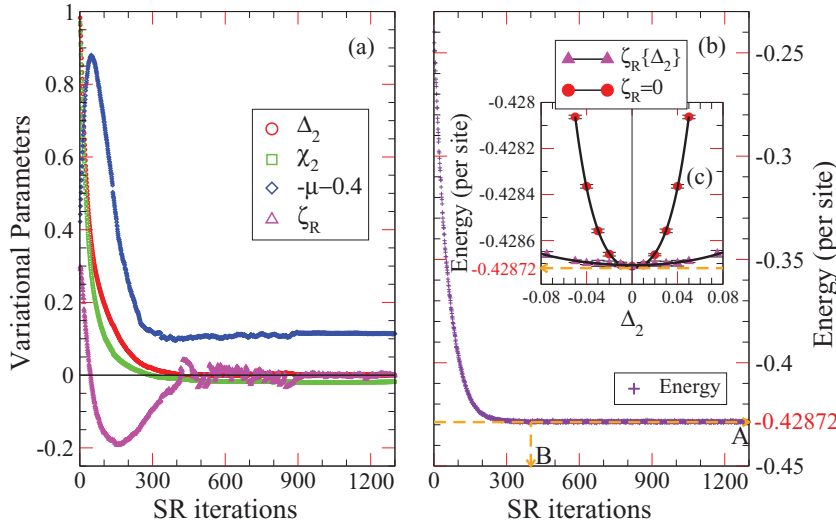


FIG. 2. (Color online) A typical variational Monte Carlo optimization run for the $\mathbb{Z}_2[0,\pi]\beta$ wave function: (a) variational parameters Δ_2 , χ_2 , μ , and ζ_R and (b) energy, as a function of SR iterations. In (a), the initialized parameter values are $\Delta_2 = \chi_2 = 1$, $\mu = -0.8$, and $\zeta_R = 0.3$. The U(1) 2nd NN $[0,\pi;0,\pi]$ Dirac SL corresponds to $\Delta_2 = 0$, $\chi_2 = -0.0186(2)$, $\zeta_R = 0$, as found in Ref. 26. The optimized parameter values are obtained by averaging over a much larger number of converged SR iterations than shown above. In (c), the variation in energy upon addition of a small Δ_2 (both for $\zeta_R = 0$, and optimized ζ_R for each value of Δ_2) upon the $[0,\pi;0,\pi]$ Dirac SL is shown, the increase in energy is apparent.

2nd NN U(1) Dirac SL, the $[0,\pi;0,\pi]$ state [see point A in Fig. 2(b)], with small but finite χ_2 [see Fig. 2(a)] previously computed by us.²⁶ For the present cluster, these values are $E/J = -0.42872(1)$ per site, and $\chi_2 = -0.0186(2)$, $\mu = -0.5124(5)$. Also, it is manifest that $(\Delta_2, \zeta_R) \rightarrow 0$, becoming exactly zero (within the error bars) after averaging over a sufficient number of converged Monte Carlo steps. Here, we bring attention to the important fact that despite the energy having converged after ≈ 400 iterations, the parameters did not converge and were still varying, converging to their final values much later than the energy (see Fig. 2). This fact is possible because, in the energy minimization, forces are calculated through the correlated sampling and not by energy differences.²⁴ Our result shows that the energy landscape along the manifold connecting the U(1) Dirac SL to the $\mathbb{Z}_2[0,\pi]\beta$ SL is *very flat* close to the U(1) Dirac SL [see Fig. 2(c) for the case $\zeta_R\{\Delta_2\}$]. Consequently, a small perturbation around the U(1) Dirac SL, e.g., by setting $\Delta_2 = 0.05$ along with the corresponding optimized value of $\zeta_R = 0.1780(2)$ will not lead to any detectable change in energy. Hence, one cannot unambiguously conclude anything about the stability of the U(1) Dirac SL by solely computing the energy of the perturbed wave function with fixed parameters, point by point locally. Only by performing an accurate SR optimization method²⁴ can one successfully optimize the parameters and transparently show that $\Delta_2 = 0$ corresponds to the actual minimum of the variational energy. This fact implies that the U(1) gauge structure is kept intact and the Dirac SL state is *locally* and *globally* stable with respect to destabilizing into the $\mathbb{Z}_2[0,\pi]\beta$ state. We verified this result by doing many optimization runs starting from different random initial values of the parameters in the four-dimensional variational space.²⁷

Regarding the remaining three gapless \mathbb{Z}_2 SLs in the neighborhood of the U(1) Dirac SL, namely, the $\mathbb{Z}_2[0,\pi]\alpha$, $\mathbb{Z}_2[0,\pi]\gamma$, and $\mathbb{Z}_2[0,\pi]\delta$ states of Ref. 21, our study reveals the same result as for the $\mathbb{Z}_2[0,\pi]\beta$ state. That is, all three of these SLs return back exactly to the gapless U(1) Dirac SL state, with the value of the parameter responsible for breaking the U(1) gauge structure down to \mathbb{Z}_2 exactly vanishing upon optimization. Thus, we can convincingly conclude that the \mathbb{Z}_2

neighborhood of the U(1) Dirac state does not contain the presumed fully gapped \mathbb{Z}_2 SL found by the DMRG study.

This conclusion forces us to shift our focus to the \mathbb{Z}_2 neighborhood of another fully symmetric (and energetically competing) gapless SL, called the uniform RVB or the $[0,0]$ SL. Despite having a slightly higher energy, it has the promising feature that all four \mathbb{Z}_2 SLs in its neighborhood are gapped, thereby opening up the possibility, albeit a slim one, that opening a gap might lead to a large gain in energy so as to make one of these four states go lower than the U(1) Dirac SL, near to the DMRG value of $E/J = -0.4379(3)$ per site. These gapped SLs are referred to in Ref. 21 as the $\mathbb{Z}_2[0,0]A$, $\mathbb{Z}_2[0,0]B$, $\mathbb{Z}_2[0,0]C$ and $\mathbb{Z}_2[0,0]D$ states; for their *Ansätze*, see Table I in Ref. 21 and also the supplementary material. Our simulations show that all four of these SLs return upon optimization to the gapless uniform RVB SL, with optimized χ_n . In particular, case by case we see that for the $\mathbb{Z}_2[0,0]A$ SL, the 2nd NN spinon pairing term goes to zero along with the on-site pairing term, thus returning back to the 2nd NN uniform RVB SL, the $[0,0;\pi,\pi]$ state given by optimized $\chi_2 = -0.032(1)$;²⁶ for the $\mathbb{Z}_2[0,0]B$ SL, the NN spinon pairing term goes to zero upon optimization, thus giving back the NN uniform RVB SL; the $\mathbb{Z}_2[0,0]C$ SL upon optimizing flows to the 3rd NN uniform RVB SL with optimized χ_2 and χ_3 s, with the spinon pairing term at 3rd NN becoming zero; and finally, the $\mathbb{Z}_2[0,0]D$ SL flows back to the 2nd NN uniform RVB SL. The results showing how the energies of these extended gapless uniform RVB SLs increase as the U(1) $\rightarrow \mathbb{Z}_2$ gauge breaking parameter is tuned on from zero to a small finite value are reported in the supplementary material (see Ref. 28).

For reasons of completeness, we mention that there are two more gapless U(1) SLs in whose neighborhoods the remaining four \mathbb{Z}_2 SLs (all gapless) lie.²¹ However, these U(1) SLs suffer from a *macroscopic* degeneracy at half-filling which leads to an open shell. This degeneracy being macroscopic cannot be removed by using any of the four real boundary condition possibilities. Hence, their energy can only be computed approximately in the limit by inserting an additional θ flux through the triangle motifs and consequently removing $\pi - 2\theta$ through hexagon motifs, and then taking the limit $\theta \rightarrow 0$. The energy of the SL- $[\pi,\pi]$ computed in

this way is $E/J \simeq -0.38372(1)$ per site, which is much higher than those of other gapless U(1) states. Hence, we did not carry out an analysis of \mathbb{Z}_2 SLs in these two neighborhoods.

Finally, we also investigated the possibility of stabilization of the $\mathbb{Z}_2[0,\pi]\beta$ state upon addition of a small 2nd NN exchange coupling (J') of both antiferromagnetic and ferromagnetic type in the NN spin-1/2 QHAF. In both cases, on optimization we found that $(\Delta_2, \zeta_R) \rightarrow 0$, becoming exactly zero (within error bars) after averaging over a sufficient number of converged Monte Carlo iterations. Thus, we recover the suitably extended, gapless 2nd NN U(1) Dirac SL. In particular, for $J'/J = 0.10$, this is the $[0,\pi;\pi,0]$ state with optimized $\chi_2 = 0.0924(2)$, and $E/J = -0.43200(2)$ per site; for $J'/J = -0.10$, this is the $[0,\pi;0,\pi]$ state with optimized $\chi_2 = -0.1066(2)$, and $E/J = -0.42898(2)$.²⁶

In summary, we investigated the possibility of stabilizing gapped \mathbb{Z}_2 SLs in the NN and next-nearest-neighbor (NNN) spin-1/2 QHAF on a kagome lattice. We found that none of the five gapped \mathbb{Z}_2 SLs [one connected to the U(1) Dirac state and the other four connected to the uniform RVB state] can occur

as ground states. In particular, the most promising gapped SL conjectured to describe the ground state, the $\mathbb{Z}_2[0,\pi]\beta$ state, is always higher in energy than the U(1) Dirac SL. Our systematic numerical results bring us to the conclusion that, at least within the Schwinger fermion approach of the spin model, the U(1) Dirac SL has the best variational energy for the NN and NNN spin-1/2 QHAF on kagome lattice. The conflict of our results, which point toward a gapless ground state, and the ones by recent DMRG calculations, which instead suggested the presence of a fully gapped spectrum, remains open and deserves further investigations. One possible direction would be to consider further improvements of our variational wave functions, based upon the application of few Lanczos steps or an approximated (fixed-node) projection technique, which, e.g., gives an energy of $E/J = -0.431453(2)$ per site for the NN U(1) Dirac SL, and $E/J = -0.431443(2)$ for the NNN $[0,\pi;0,\pi]$ state. Another possible direction would be to explore the energetics of gapped \mathbb{Z}_2 SLs which break some symmetries such as time-reversal. The possibility that the fully gapped SL found by the DMRG study possesses a different low energy gauge structure other than \mathbb{Z}_2 also remains open.

¹J. B. Marston and C. Zeng, *J. Appl. Phys.* **69**, 5962 (1991).

²M. B. Hastings, *Phys. Rev. B* **63**, 014413 (2000).

³P. Nikolic and T. Senthil, *Phys. Rev. B* **68**, 214415 (2003).

⁴R. R. P. Singh and D. A. Huse, *Phys. Rev. B* **76**, 180407(R) (2007).

⁵D. Poilblanc, M. Mambrini, and D. Schwandt, *Phys. Rev. B* **81**, 180402(R) (2010); D. Schwandt, M. Mambrini, and D. Poilblanc, *ibid.* **81**, 214413 (2010).

⁶P. W. Anderson, *Mater. Res. Bull.* **8**, 153 (1973).

⁷P. W. Anderson, *Science* **235**, 1196 (1987).

⁸S. Yan, D. A. Huse, and S. R. White, *Science* **332**, 1173 (2011).

⁹A. Olariu, P. Mendels, F. Bert, F. Duc, J. C. Trombe, M. A. de Vries, and A. Harrison, *Phys. Rev. Lett.* **100**, 087202 (2008).

¹⁰F. Bert, S. Nakamae, F. Ladieu, D. L'Hôte, P. Bonville, F. Duc, J.-C. Trombe, and P. Mendels, *Phys. Rev. B* **76**, 132411 (2007).

¹¹P. Mendels, F. Bert, M. A. de Vries, A. Olariu, A. Harrison, F. Duc, J. Trombe, J. Lord, A. Amato, and C. Baines, *Phys. Rev. Lett.* **98**, 077204 (2007).

¹²T. Imai, E. A. Nytko, B. M. Bartlett, M. P. Shores, and D. G. Nocera, *Phys. Rev. Lett.* **100**, 077203 (2008).

¹³O. Ofer, A. Keren, E. A. Nytko, M. P. Shores, B. M. Bartlett, D. G. Nocera, C. Baines, and A. Amato, e-print arXiv:cond-mat/0610540).

¹⁴J. S. Helton, K. Matan, M. P. Shores, E. A. Nytko, B. M. Bartlett, Y. Yoshida, Y. Takano, A. Suslov, Y. Qiu, J.-H. Chung, D. G. Nocera, and Y. S. Lee, *Phys. Rev. Lett.* **98**, 107204 (2007).

¹⁵S.-H. Lee, H. Kikuchi, Y. Qiu, B. Lake, Q. Huang, K. Habicht, and K. Kiefer, *Nat. Mater.* **6**, 853 (2007).

¹⁶M. A. de Vries, K. V. Kamenev, W. A. Kockelmann, J. Sanchez-Benitez, and A. Harrison, *Phys. Rev. Lett.* **100**, 157205 (2008).

¹⁷D. Wulferding, P. Lemmens, P. Scheib, J. Röder, P. Mendels, S. Chu, T. Han, and Y. S. Lee, *Phys. Rev. B* **82**, 144412 (2010).

¹⁸Y. Ran, M. Hermele, P. A. Lee, and X.-G. Wen, *Phys. Rev. Lett.* **98**, 117205 (2007).

¹⁹M. Hermele, Y. Ran, P. A. Lee, and X.-G. Wen, *Phys. Rev. B* **77**, 224413 (2008).

²⁰Xiao-Gang Wen, *Phys. Rev. B* **65**, 165113 (2002).

²¹Y.-M. Lu, Y. Ran, and P. A. Lee, *Phys. Rev. B* **83**, 224413 (2011).

²²T. Tay and O. I. Motrunich, *Phys. Rev. B* **84**, 020404(R) (2011).

²³X. G. Wen, *Phys. Rev. B* **44**, 2664 (1991).

²⁴S. Sorella, *Phys. Rev. B* **71**, 241103(R) (2005).

²⁵S. Yunoki and S. Sorella, *Phys. Rev. B* **74**, 014408 (2006).

²⁶Y. Iqbal, F. Becca, and D. Poilblanc, *Phys. Rev. B* **83**, 100404(R) (2011).

²⁷We also verified the same, by using the original non-gauge-transformed representation of the $\mathbb{Z}_2[0,\pi]\beta$ Ansatz, as given in Table I of Ref. 21.

²⁸See Supplemental Material at <http://link.aps.org/supplemental/10.1103/PhysRevB.84.020407> for more information.